

# Effect of Molecular Interactions on Gas Permeation Properties through a Microporous Silica Membrane Studied with Molecular Dynamics Simulation

Tomohisa Yoshioka, Toshinori Tusru and Masashi Asaeda

Department of Chemical Engineering, Hiroshima University,

Higashi-Hiroshima, 739-8527, Japan

Fax: 81-82-424-5494, e-mail: tom@hiroshima-u.ac.jp

Non-equilibrium molecular dynamics simulations of gas permeation through a sub-nano scale pore were conducted on a virtual amorphous silica membrane. Effects of the molecular interactions on gas permeation properties were examined through the studies of temperature and pressure dependencies for permeance. Some types of imaginary LJ particles were used to simulate condensable or non-condensable gas permeation. Concerning the permeation properties of the CO<sub>2</sub>-like LJ particle through a pore of 6 Å in diameter, a surface diffusion-like temperature dependency was observed at relatively high temperature region (400-800 K). In the simulations using molecules, which have larger interaction with the silica framework, the permeance became greater in high temperature region, and the slight decreasing tendency at lower temperature region could be seen. The maximum peak in a temperature dependency curve of permeance was more clearly observed when a larger intermolecular interaction parameter was adopted. A decrease in diffusivity around room temperature was also indicated in the case of larger interaction among permeants and higher downstream pressure through the study of MSD calculations. The formation of micropore filling phase of permeating condensable molecules would have an important role to determine the permeation properties through a micropore.

Key words: molecular dynamics, silica membrane, micropore, gas permeation

## 1. INTRODUCTION

Gas separation processes which utilize microporous inorganic membranes appear to be a very promising technology. The recent remarkable development of a variety of porous inorganic membranes such as sol-gel derived ceramic membranes, CVD modified membranes, and zeolite membranes has enabled the separation of specific components from molecular mixtures. Since those porous inorganic membranes have relatively good chemical and thermal resistance, they would be expected to be useful under severe conditions. For example, applications to the separation of hydrogen from organic gas mixtures in industrial chemical processes [1] and carbon dioxide separation from methane or nitrogen etc. could be attained [2]. In order to design a porous inorganic membrane unit and to determine the optimized operating conditions for those separation processes, knowledge of the transport mechanisms of molecules within micropores is indispensable.

The mechanism of gas permeation for microporous inorganic membranes has been studied using zeolite or modified glass membranes by many researchers [3-5]. We have also reported for the gas phase permeation at relatively high temperatures [2] and vapor permeation at temperatures below  $T_c$  (critical

temperature) [6]. However, the dependency of permeation properties of molecules on the nature of permeating molecules such as molecular size and interaction parameters is not still clear.

In this study, we prepared a virtual amorphous silica membrane which had a pore of sub-nanometer in diameter on a computer, and employed a simple Non-Equilibrium Molecular Dynamics (NEMD) simulation scheme for the observation of gas permeation phenomena. By using the MD simulation as an ideal experimental system, microporous membranes of any desired pore size and some virtual permeating molecules can be prepared on a computer and the permeation behavior can be observed from a microscopic point of view. Simulated permeation properties were analyzed based on gas permeation models. The bulk properties such as critical temperature and saturation pressure of virtual permeants were also calculated and considered in qualitative understanding of permeation mechanisms.

## 2. NEMD SIMULATION METHOD

The system used in the simulations consisted of a membrane unit cell which had a sub-nano scale pore and permeating gas or vapor molecules. The membrane material was amorphous silica which consisted of Silicon and Oxygen atoms,

and the permeating gas molecules were He and CO<sub>2</sub>-like LJ particles. In order to simulate the amorphous silica structure, we employed the modified BMH (Born-Mayer-Huggins) pair potential and the SW (Stillinger-Weber) 3-body potential [7]. For interactions among permeating molecules and between permeating molecules and oxygen atoms on the membrane, the widely known Lennard-Jones potential given by Eq. (1) was used.

$$E(r_{ij}) = 4\epsilon_{ij} \left[ \left( \frac{\sigma_{ij}}{r_{ij}} \right)^{12} - \left( \frac{\sigma_{ij}}{r_{ij}} \right)^6 \right] \quad (1)$$

A virtual amorphous SiO<sub>2</sub> membrane was initially prepared using melt-quench procedures [7]. Details of the procedures were the same as that reported elsewhere [8]. The resulting membrane unit cell was about 28.5 Å in length for the *x*, *y*, and *z* directions, that is the length of the pore or the thickness of the membrane was 28.5 Å. This unit cell had a cylindrical 6 Å pore in diameter, passing through it in *z*-direction.

In order to carry out a non-equilibrium MD simulation under constant pressure and temperature, we introduced a boundary plane with an imaginary gas phase [8], on which the permeating gas particles could be produced or deleted. This setting allowed us to maintain pressure gradient across a membrane unit with the given upstream and downstream pressure. The initial velocity of molecules produced at the boundary plane could be reasonably given based on the kinetic theory of ideal-gases as well as the frequency of molecular production. The forces acting on the permeating molecules in a pore result from permeant-permeant molecular and permeant-“silica framework” interactions. Permeating molecules were assumed to interact with oxygen atoms on silica and forces originating from silicon atoms were neglected. To obtain ‘permeant-O’ potential parameters, the Lorentz-Berthelot combining rules were used. The Lennard-Jones potential parameters used in our simulations are summarized in Table 1, where b-O and nb-O indicate bridging oxygen (Si-O-Si) and non-bridging oxygen (Si-OH), respectively. We proceeded with the simulations of the dynamics, not only of permeating molecules but also of Si and O atoms on a silica membrane. An MD time step of 1 fs was used with the fifth order Gear’s algorithm for integrating Newton’s equations of motion.

Table I Lennard-Jones potential parameters

$\epsilon_{\text{gas}} / k$ [K]	10.22 (He), 49, 195 (CO <sub>2</sub> ), 293
$\epsilon_{\text{gas-solid}} / k$ [K]	48.5 (He), 212, 300
$\sigma_{\text{gas}}$ [Å]	2.6 (He), 3.3 (CO <sub>2</sub> )
$\sigma_{\text{solid}} (\text{b-O})$ [Å]	2.7
$\sigma_{\text{solid}} (\text{nb-O})$ [Å]	3.0

*k*: Boltzmann constant

In a measurement of the temperature dependency

of permeance (molecules·s<sup>-1</sup>·Pa<sup>-1</sup>), the upstream pressure, *p*<sub>u</sub> was 2 MPa and the downstream pressure, *p*<sub>d</sub> was zero MPa. The temperatures used were from 260 to 800 K. The bulk critical temperatures and saturation pressures of permeating molecules were also calculated.

### 3. RESULTS AND DISCUSSION

#### 3.1 Gas Permeation models

In general, permeation flux, *J*, in the direction of *x* can be given by widely known Eq. (2) [3],

$$J = -Bc \frac{d\mu}{dx} = -D' \frac{d \ln p}{d \ln c} \frac{dc}{dp} \frac{dp}{dx} \quad (2)$$

where,  $\mu$  is chemical potential, *B* mobility, *c* concentration, and *D*’ corrected diffusion coefficient, which is a function of geometrical factors, the mean molecular velocity and the mean free path. The permeance, *P*, can be given using the apparent pressure drop  $\Delta p$  and the diffusion length *L* by  $P = JL / \Delta p$ . In the case of the permeation of non-adsorptive molecules, we have the Knudsen formula, Eq. (3),

$$P_K = \frac{k_g}{(MRT)^{0.5}} \quad (3)$$

while, if the relation between *c* and *p* can be described as  $cRT = p \exp(-E_p/RT)$ , Eq. (4) can be obtained from Eq. (2) as well [2],

$$P_p = \frac{k_g}{(MRT)^{0.5}} \exp\left(-\frac{E_p}{RT}\right) \quad (4)$$

where, *E*<sub>p</sub> is a potential in a micropore through which permeating molecules are transported. In the gas permeation at relatively low temperature and high pressure conditions, the Langmuir type relation between *c* and *p* given by Eq. (5) is one of the good descriptions for a gas permeation model.

$$c = \frac{abp}{1+ap} \quad (5)$$

*b* is adsorption capacity per unit volume in a micropore. *a* is proportional to the adsorption rate, and it can be expressed as an Arrhenius equation using adsorption energy based on statistical thermodynamics, and *c* can be assumed to be equal to *abp* at the limit of *p* = 0. Therefore, the parameter, *a*, could be expressed approximately by Eq. (6).

$$a = \frac{\exp(-E_p/RT)}{bRT} \quad (6)$$

From Eqs. (2), (5) and (6), we have Eq. (7) as the expression of permeance, *P*<sub>L</sub> [8],

$$P_L = \frac{k_g}{(MRT)^{0.5}} \frac{\exp(-E_p/RT)}{1 + \frac{p_m}{bRT} \exp(-E_p/RT)} \quad (7)$$

where, *p*<sub>m</sub> is the mean pressure across a membrane.

#### 3.2 Simulated Gas Permeation properties

Fig. 1 shows snapshots of gas permeation simulations of He and CO<sub>2</sub>-like LJ particles at 300 K through a pore of 6 Å. The upper- and downstream pressures are 2 and zero MPa, respectively. The energy parameter of He is

relatively small and it has little interaction with each other and the pore surface. He particles appeared to permeate as normal gas molecules. On the contrary, the concentrations of CO<sub>2</sub>-like particles in the pore are larger than that of He, and the concentration of particles in a pore became obviously larger when larger energy parameter was adopted. These results suggest that not only interactions between permeating molecules and the pore surface but those among permeating molecules may play an important role in determining the permeation properties through a micropore as well.

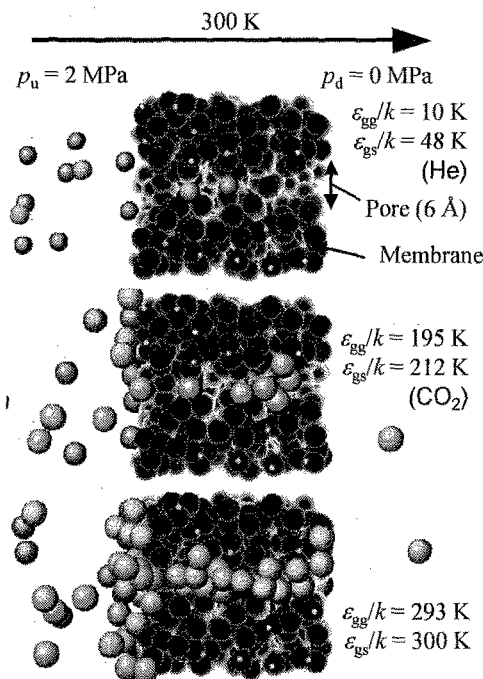


Fig. 1 Snapshots of a cross-sectional view of a membrane and permeating He and CO<sub>2</sub>-like particles at 300 K;  $p_u = 2$  MPa,  $p_d = 0$  MPa.

Fig. 2 shows the Arrhenius plots of permeance for He and CO<sub>2</sub>-like particles. The temperature dependency for He permeance was not so striking and was almost the same as the Knudsen's slope. On the contrary CO<sub>2</sub>-like particles showed obviously larger temperature dependency, and those data could be well fitted with Eq. (7). At temperatures above 400 K, Eq. (4) could also well explain the simulated permeance and this indicates gas phase permeation enhanced by attractive interaction with the pore surface, which is generally recognized as 'surface diffusion'. When the interaction parameter between a permeating molecule and the pore surface,  $\epsilon_{gs}/k$  increased from 212 K to 300 K, the permeances at high temperature region became greater, while, at temperatures below 300 K, the permeance slightly decreased with decreasing temperature and was nearly same as that of  $\epsilon_{gs}/k = 212$  K particle at 300 and 260 K.

Fig. 3 shows the Arrhenius plots of permeance for virtual particles whose intermolecular parameters,  $\epsilon_{gg}/k$  are 49, 195 and 293 K. Those temperature dependency

curves are nearly identical in high temperature region, which indicates gas state permeation independent of the intermolecular interaction. On the contrary, the curve of  $\epsilon_{gg}/k = 293$  K particle at low temperature region cannot be explained by the Langmuir-type permeation model described by Eq. (7). Larger intermolecular interactions and resulting filling phenomenon of permeating molecules might prevent them from moving as gas phase in a micropore, and this would lead to decrease permeance at low temperatures.

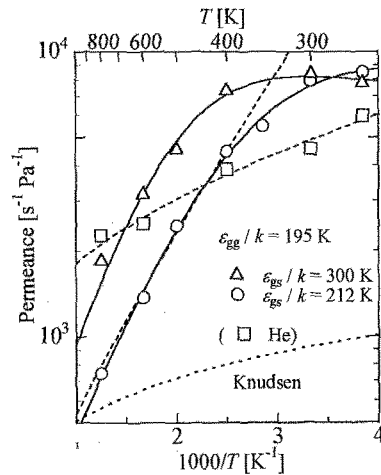


Fig. 2 Dependencies of permeance on temperature and affinity with pore surface. Solid curves are fitted with Eq. (7) and broken ones Eq. (4);  $p_u = 2$  MPa,  $p_d = 0$  MPa.

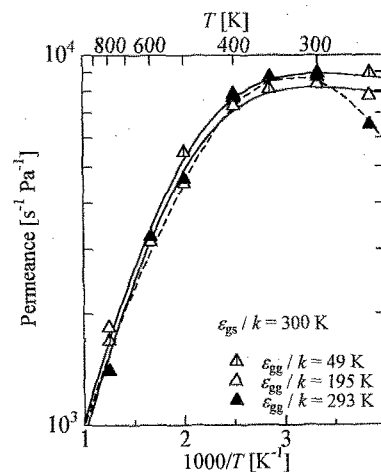


Fig. 3 Dependencies of permeance on temperature and intermolecular interaction. Solid curves are fitted with Eq. (7) and broken one a guide for eye;  $p_u = 2$  MPa,  $p_d = 0$  MPa.

### 3.3 Bulk properties of a virtual particle

In order to investigate the bulk properties of  $\epsilon_{gg}/k = 293$  K particle such as a critical temperature,  $T_c$  and a saturation pressure,  $p_s$ ,  $NVT$  MD simulations for dynamical liquid-gas equilibrium were conducted. Fig. 4 shows the density profiles in a MD simulation cell at several temperatures. High density part and lower one correspond to liquid phase and gas phase, respectively. The abrupt decrease of density indicates the existence of a liquid-gas interface

and this means that the temperature might be lower than  $T_C$ . Therefore, the value of  $T_C$  for this particle could be estimated as 300 to 350 K from the figure. This value is nearly equal to a temperature where the maximum of permeance was observed in Fig.3. This is very suggestive for permeation of condensable gases through a micropore. At temperatures below  $T_C$ , permeating gas or vapor molecules could easily form a liquid-like high density phase when the pressure outside is sufficiently high. The value of  $p_s$  for this particle at 260 K estimated from the *NVT* MD simulation was 3.1 MPa, and a micropore filling pressure [6],  $p_f$  estimated from the Polanyi's adsorption potential theorem given by Eq. (8) was 0.03 MPa, which was indeed lower than the upstream pressure of 2 MPa.

$$E_p = RT \ln \left( \frac{p_f}{p_s} \right) \quad (8)$$

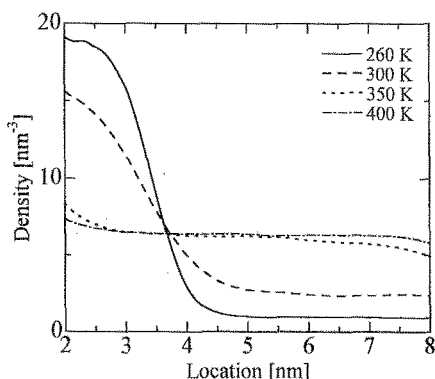


Fig. 4 Density profiles around gas-liquid interface for  $\epsilon_{gg}/k=293$  K particle at 260, 300, 350 and 400 K

#### 3.4 Mobility of molecules within a micropore

The mobility of molecules in a micropore under several operating conditions was investigated by calculating the mean-square displacements (MSD) in adsorption ( $p_u = p_d = 1.5$  MPa) and permeation ( $p_u = 2$  MPa,  $p_d = 1$  and 0 MPa) simulations. The results are shown in Fig. 5. The slope of the MSD curve corresponds to the diffusion coefficient. Therefore, it can be seen that the mobility of  $\epsilon_{gg}/k=49$  K particle is greater than that of  $\epsilon_{gg}/k=293$  K particle in the micropore filling phase. An increase in operating downstream pressure also decreased the diffusivity of permeating molecules in the pore as well. These results suggest that the decrease in permeance of condensable permeants under low temperature or high pressure conditions would be related to the formation of a micropore filling phase within sub-nano scale pores, and the larger intermolecular interaction could more strongly obstruct the transport in a micropore filling phase.

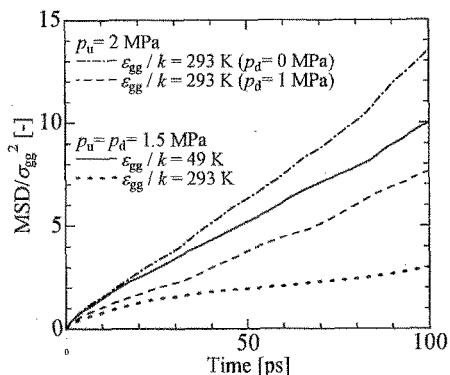


Fig. 5 Mean square displacement curves at 300 K.

#### 4. CONCLUSION

A virtual amorphous silica membrane that had a sub-nano scale pore was prepared, and gas or vapor permeation simulations were conducted using a simple NEMD method. The temperature dependencies of permeance for CO<sub>2</sub>-like virtual particles were calculated, and the effect of the affinity of permeating molecules with the pore surface and intermolecular interactions among permeants on their permeation properties were studied. Surface diffusion-like temperature dependencies were observed at relatively high temperature region, while around 300 K, near the critical temperature of actual CO<sub>2</sub>, the permeance decreased with decreasing temperature. In the simulations using molecules, which have larger interaction with the pore surface, the permeance became greater in high temperature region, while a slight decreasing tendency at lower temperature region could be observed. The maximum peak in a temperature dependency curve for permeance was more obvious when a larger interaction parameter among permeating molecules was adopted. As confirmed in MSD calculations, the formation of micropore filling phase of permeating molecules within a micropore facilitated by larger intermolecular interaction and higher operating pressure would decrease the permeation rate.

#### REFERENCES

- [1] K. Yoshida, Y. Hirano, H. Fujii, T. Tsuru and M. Asaeda, *J. Chem. Eng. Jpn.* **34**, 523-530 (2001).
- [2] T. Yoshioka, E. Nakanishi, T. Tsuru and M. Asaeda, *AIChE J.* **47**, 2052-2063 (2001).
- [3] A. B. Shelekhin, A. G. Dixon and Y. H. Ma, *AIChE J.* **41**, 58-67 (1995).
- [4] A. J. Burggraaf, *J. Mem. Sci.* **155**, 45-65 (1999).
- [5] J. C. Poshusta, R. D. Noble and J. L. Falconer, *J. Mem. Sci.* **160**, 115-125 (1999).
- [6] T. Yoshioka, T. Tsuru and M. Asaeda, *Sep. and Purif. Technol.* **32**, 231-237 (2003).
- [7] B. P. Feuston and S. H. Garofalini, *J. Chem. Phys.* **89**, 5818-5824 (1988).
- [8] T. Yoshioka, T. Tsuru and M. Asaeda, *Sep. and Purif. Technol.* **25**, 441-449 (2001).